


Broadband and stable acoustic vortex emitter with multi-arm coiling slits

Cite as: Appl. Phys. Lett. **108**, 203501 (2016); <https://doi.org/10.1063/1.4949337>

Submitted: 26 January 2016 . Accepted: 29 March 2016 . Published Online: 16 May 2016

Xue Jiang, Jiajun Zhao, Shi-lei Liu, Bin Liang, Xin-ye Zou, Jing Yang, Cheng-Wei Qiu, and Jian-chun Cheng 



View Online



Export Citation



CrossMark

ARTICLES YOU MAY BE INTERESTED IN

[Particle manipulation with acoustic vortex beam induced by a brass plate with spiral shape structure](#)

Applied Physics Letters **109**, 123506 (2016); <https://doi.org/10.1063/1.4963185>

[Making sound vortices by metasurfaces](#)

AIP Advances **6**, 085007 (2016); <https://doi.org/10.1063/1.4961062>

[Generation of topologically diverse acoustic vortex beams using a compact metamaterial aperture](#)

Applied Physics Letters **108**, 223503 (2016); <https://doi.org/10.1063/1.4953075>

Lock-in Amplifiers
Find out more today



 Zurich Instruments



Broadband and stable acoustic vortex emitter with multi-arm coiling slits

Xue Jiang,^{1,2,a)} Jiajun Zhao,^{3,4,a)} Shi-lei Liu,¹ Bin Liang,^{1,2,b)} Xin-ye Zou,^{1,2} Jing Yang,^{1,2} Cheng-Wei Qiu,^{5,b)} and Jian-chun Cheng^{1,2,b)}

¹Key Laboratory of Modern Acoustics, MOE, Institute of Acoustics, Department of Physics, Nanjing University, Nanjing 210093, People's Republic of China

²Collaborative Innovation Center of Advanced Microstructures, Nanjing University, Nanjing 210093, People's Republic of China

³Department of Physics and Center for Nonlinear Dynamics, University of Texas at Austin, Austin, Texas 78712, USA

⁴Division of Computer, Electrical and Mathematical Sciences and Engineering, King Abdullah University of Science and Technology (KAUST), Thuwal 23955-6900, Saudi Arabia

⁵Department of Electrical and Computer Engineering, National University of Singapore, Singapore 117576, Singapore

(Received 26 January 2016; accepted 29 March 2016; published online 16 May 2016)

We present the analytical design and experimental realization of a scheme based on multi-arm coiling slits to generate the stable acoustic vortices in a broadband. The proposed structure is able to spiral the acoustic wave spatially and generate the twisted acoustic vortices with invariant topological charge for a long propagation distance. Compared with conventional methods which require the electronic control of a bulky loudspeaker, this scheme provides an effective and compact solution to generate acoustic vortices with controllable topological charge in the broadband, which offers more initiatives in the demanding applications. *Published by AIP Publishing.*

[<http://dx.doi.org/10.1063/1.4949337>]

Acoustic vortices, imprinted with the orbital angular momentum (OAM), have demonstrated theoretical and experimental importance in recent decades.^{1–3} One typical characteristic of the acoustic vortices is the helical dislocation of the wave front which is described by an azimuthal θ phase dependence $\exp(im\theta)$.^{4,5} The integer number m is called the topological charge, corresponding to the order of the vortex, which determines the total phase accumulated in one full annular loop around the propagation axis. Another property of the acoustic vortices is the indeterminate phase and null pressure magnitude at the core of vortices, which is useful for trapping and manipulating particles smaller than wavelength, through controlling and moving position of the central vortex null.^{6–8} Moreover, OAM of acoustic vortices can generate a rotation torque, resulting in the acoustic radiation force, which provides the possibility to manipulate the rotation of microscopic objects in the acoustic field.^{9,10}

All these intriguing properties of acoustic vortices have spurred many efforts to generate them with well-developed and neoteric vortex generators. For example, Hefner and Marston used the acoustic source with a radiating surface to generate the acoustic vortex and found the ratio of the axial angular momentum flux to the acoustical beam power in 1998.¹¹ Then they constructed and evaluated another scheme with an array of individually addressed acoustic transducers excited with appropriate phases to produce the ultrasonic vortex,¹² which serves as the most common method to generate the acoustic vortices thereafter.^{13–15} Further achievements have been made on the research of acoustic vortices based on the sparsely distributed acoustic transducer array,

such as the experimental observation of fluid rotation driven by an acoustic vortex,¹⁶ transferring OAM from acoustic vortex to microparticle¹⁷ and so on.¹⁸ In principle, acoustic vortex can be boundlessly generated by the complex electronic-based acoustic transducer array, or called the active method. However, the active method has some drawbacks which would weaken its potential in practice. From a technical point of view, the traditional active method requires the electronic control of individual pixel of the transducer array to provide the appropriate phase and amplitude, which is costly in practice. On the other hand, the acoustic loudspeaker or transducer employed as the individual element of the array is always with the finite dimensions comparable with the acoustic wavelength. The limitation of the discretization precision would significantly restrict the miniaturization and employment for MEMS applications of such electronic controlled device. It is desirable to pursue an alternative controllable acoustic vortices generator, exempted from the complicate electronic control, endowed with the invariant topological charge and smaller scale.

In this paper, we report on the analytical design, numerical simulation, and experimental realization of an acoustic vortices generator based on the multi-arm coiling slits (MACS) in a broadband. The MACS-based generator has the ability to produce the twisted stable acoustic vortices by modulating the amplitude and phase of waves in the diffraction field. The stability and sustenance of the topological charge can be extended to a long distance in the propagation direction for all the cases of one-armed to four-armed coiling slits. Remarkably, the MACS has the intrinsic broadband functionality due to the absence of resonate components, which would be of significant importance in practice. The generation of acoustic vortex with the topological charge $m = 1$ and $m = 4$ are presented by the one-armed and four-armed MACS,

^{a)}Xue Jiang and Jiajun Zhao contributed equally to this work.

^{b)}Authors to whom correspondence should be addressed. Electronic addresses: liangbin@nju.edu.cn; eleqc@nus.edu.sg; and jccheng@nju.edu.cn

respectively, in two arbitrary frequency (425 kHz and 625 kHz), and the agreements are observed between the predictions and experimental measurements. Without complicated electronic control and the limitation of the discretization precision, the MACS-based scheme provides an effective and compact solution to generate the acoustic vortices with controllable topological charge in a broadband.

The schematic diagram of the working principle of the MACS for generating the stable acoustic vortices is illustrated in Fig. 1. For simplicity while without losing generality, we consider the one-armed coiling slit for producing the acoustic vortex with the topological charge $m = 1$ to demonstrate the working principle, and results of vortices with other topological charge by other MACS can be obtained in a similar manner. The one-armed coiling slit is enclosed with two logarithmic spiral curves, and the overall structural parameters of the two curves are expressed in the polar coordinates $r = a_1 e^{b\theta}$ and $r = a_2 e^{b\theta}$, respectively, with r being the radial coordinate and θ being the angular coordinate. The factor $a_1 = 13.8$ mm and $a_2 = 14.85$ mm are the initial radii of the two spiral curves whereas azimuthal factor $b = 0.0225$ determines the growth rate of rotation, and the two spiral curves growth from $\theta_1 = 0$ to $\theta_2 = 12\pi$. In Fig. 1 the dark gray region is hollow and the light gray part is constructed with rigid material. Therefore, when an acoustic plane wave impinges on the plate, only the wave in the spiral region can be transmitted and others which interacted with the rigid surface would be reflected back. In other words, the impressed MACS can be regarded as a binary-amplitude mask.

For theoretical interpretation, Rayleigh–Sommerfeld diffraction integral is applied to calculate the acoustic pressure in the viewing point $Q(\rho, \varphi, z)$, where ρ and φ are, respectively, the radial and azimuthal coordinates at the observation plane and z is the distance between the structure and observation plane. The normalized pressure at the viewing point Q is governed by

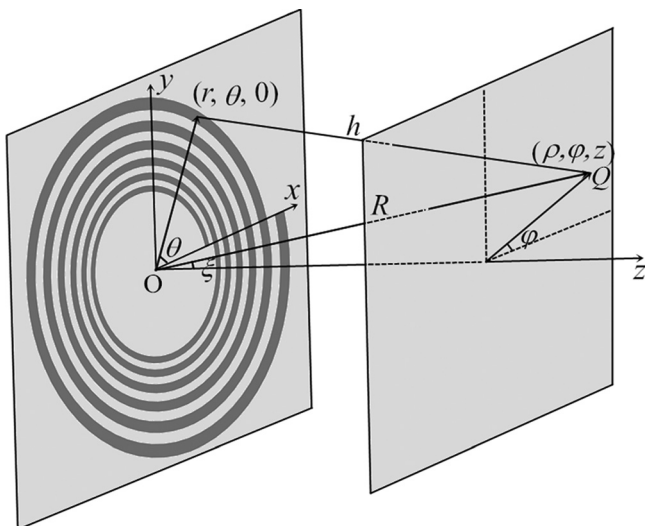


FIG. 1. Diagram of the working principle of the multi-arm coiling slits for generating the stable acoustic vortices. Dark gray indicates the hollow region.

$$p_1(\rho, \varphi, z) = \int_{\theta_1}^{\theta_2} \int_{a_1 e^{b\theta}}^{a_2 e^{b\theta}} \frac{i\omega\rho_0}{2\pi h} e^{i(\omega t - kh)} r dr d\theta, \quad (1)$$

where ω and k are the angular frequency and wave number of the incident wave, ρ_0 is the mass density of the background material, $h = \sqrt{\rho^2 + r^2 + z^2 - 2rR \cos \varphi \sin \xi}$ is the distance between the viewing point and the point in the structure, $R = \sqrt{\rho^2 + z^2}$ is the distance between point Q and the origin point O , and $\xi = \arctan(\rho/z)$ is the angle between point Q and the z axis. Therefore the diffraction field after the one-armed coiling slit can be acquired by Eq. (1). The initial radii and azimuthal angle of the other three MACS are the same as the one-armed structure, i.e., $a_1 = 13.8$ mm, $a_2 = 14.85$ mm, and $\theta_1 = 0$, while other structural parameters are $b = 0.0451$, $\theta_2 = 6\pi$ for the two-armed coiling slit, $b = 0.0676$, $\theta_2 = 4\pi$ for the three-armed design, and $b = 0.0902$, $\theta_2 = 3\pi$ for the four-armed case. Schematics of the one-armed to four-armed coiling slits are shown in the first row of Fig. 2. For other MACS, the corresponding diffraction fields can be obtained by superposing pressures from individual arms, and the total pressure after the m -armed structure is described as follows:

$$p_m(\rho, \varphi, z) = \sum_{n=1}^m \int_{\theta_1}^{\theta_2} \int_{a_1 e^{b[\theta + 2\pi(n-1)/m]}}^{a_2 e^{b[\theta + 2\pi(n-1)/m]}} \frac{i\omega\rho_0}{2\pi h} e^{i(\omega t - kh)} r dr d\theta. \quad (2)$$

Performances of the designed MACS to generate the stable acoustic vortices with different topological charges are demonstrated via numerical simulations first. Throughout the paper, the finite element method based on COMSOL Multiphysics software is used for the numerical simulations; the background medium is chosen as water whose mass density and sound speed are 1000 kg/m^3 and 1500 m/s , respectively; and the material of the spiral plates is set to be rigid, whose acoustic impedance is much larger than that of water. A summary of the simulated phase and normalized intensity distributions (normalized with the corresponding maximums) of the one-armed to four-armed coiling slit in 425 kHz at the cross-sections $z = 2.5\lambda$ are illustrated in the second and third rows of Fig. 2, respectively, where λ is the wavelength of the incident acoustic wave. The performance of the structures in different frequencies and propagation distances will be demonstrated in the following paragraph. It can be observed that the phases have changed 2π , 4π , 6π , and 8π in an annular loop of the diffraction phase fields generated by the one-armed to four-armed structures, which proves that the topological charges of the acoustic vortices are $m = 1$, $m = 2$, $m = 3$, and $m = 4$, respectively.

Experiments are designed and carried out to verify the generation of the broadband stable acoustic vortices by the proposed MACS in practice. For simplicity while without losing generality we demonstrate the performance of the coiling slits with the minimum and maximum arms to show the validity of the structure. Figures 3(a) and 3(b) are the photographs of the samples of the one-armed and four-armed coiling slits. The samples are fabricated via the three-dimensional metal printing technology. The material of the samples is chosen to be 17–4ph stainless steel, whose mass density and sound speed are 7800 kg/m^3 and 5000 m/s , respectively. The acoustic

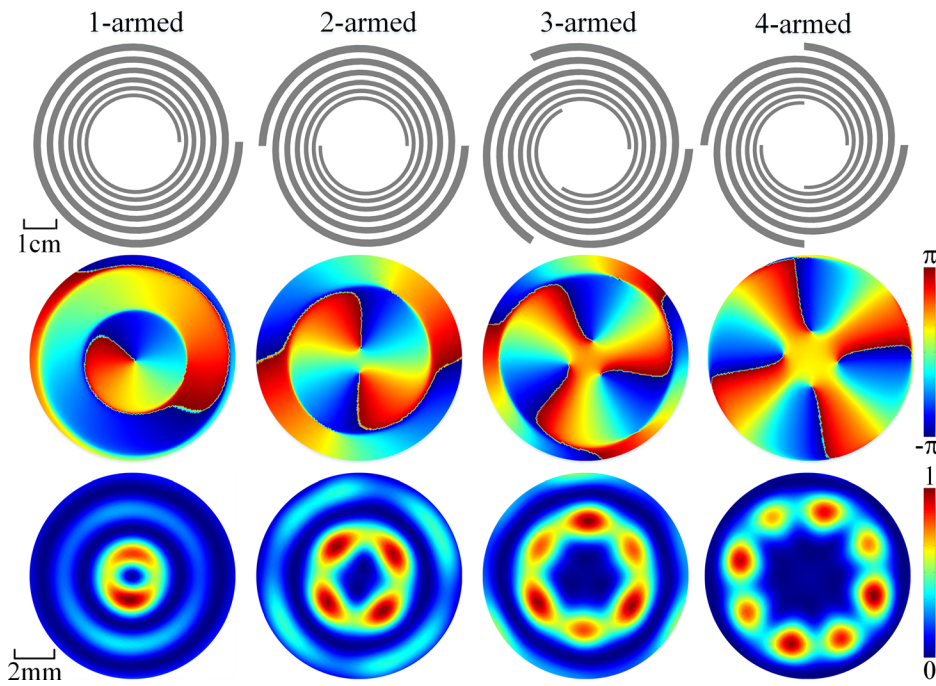


FIG. 2. Summary of the schematic of the one-armed, two-armed, three-armed, and four-armed MACSs (first line), simulated phase (second line), and normalized acoustic intensity (third line) distributions in 425 kHz at the cross-section $z = 2.5\lambda$.

impedance of the steel is $3.9 \times 10^7 \text{ N s/m}^3$, which is about 26 times as that of water; therefore, it is reasonable to regard the 17–4 ph stainless steel as a kind of rigid material in water. The experimental setup is schematically illustrated in Fig. 3(c). An unfocused ultrasonic transducer with the diameter of 4.2 cm and central frequency of 500 kHz is employed to produce the incident field. A harmonic signal is generated by the signal function generator (Agilent 33250A), going through the amplifier (Electronics & Innovation, Model: 2200L) and reaching the transducer. The transducer is placed 20 cm away from the surface of the sample to mimic a good plane wave source in water tank, and a moveable hydrophone (ONDA HNC-1000) is employed to scan the pressure fields after the sample. All devices are submerged in the deaerated water produced by ONDA Water Conditioner (Model: MECS220). With the help of computer, the ultrasonic signals are recorded and processed. The experimental results for the one-armed and four-armed structures in 425 kHz at the cross-section $z = 2.5\lambda$ are shown in Figs. 3(d) and 3(e). The phases have shifted from $-\pi$ to π for one time and four times in an annular loop for the

one-armed and four-armed structures, respectively, which clearly shows that the topological charges of the corresponding generated acoustic vortices is $m = 1$ and $m = 4$. Good agreements are observed between the simulations (Fig. 2) and measurements (Fig. 3), which verifies that the generation of the stable acoustic vortices by the proposed MACSs is experimentally validated.

Remarkably, it is noteworthy that the diffracted wave is designed to propagate with a stable phase profile, and the topological charge of each structure should be invariant at different propagation distances. Moreover, the MACS should have the intrinsic broadband functionality since the generation is driven by the diffraction effect of the delicately designed spiral structures and no resonant component is required in the structure. In fact, the only restriction on the bandwidth lies in the largest and smallest slit widths d_{\max} and d_{\min} of the slit. As long as the wavelength of the incident wave λ is in the range of $[0.5d_{\max}, 0.5d_{\min}]$ for allowing the effective diffraction, the proposed MACS is able to generate the acoustic vortices in accordance with the expectation. For

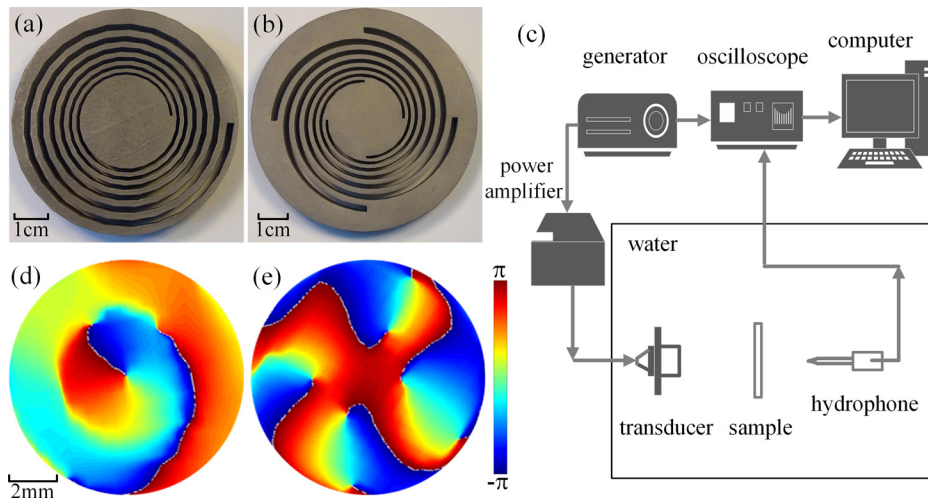


FIG. 3. (a) and (b) Photographs of the one-armed and four-armed MACS samples. (c) Schematic of the experimental setup. (d) and (e) Experimental measurements of the phase distributions for the one-armed and four-armed MACS in 425 kHz at the cross-section $z = 2.5\lambda$.

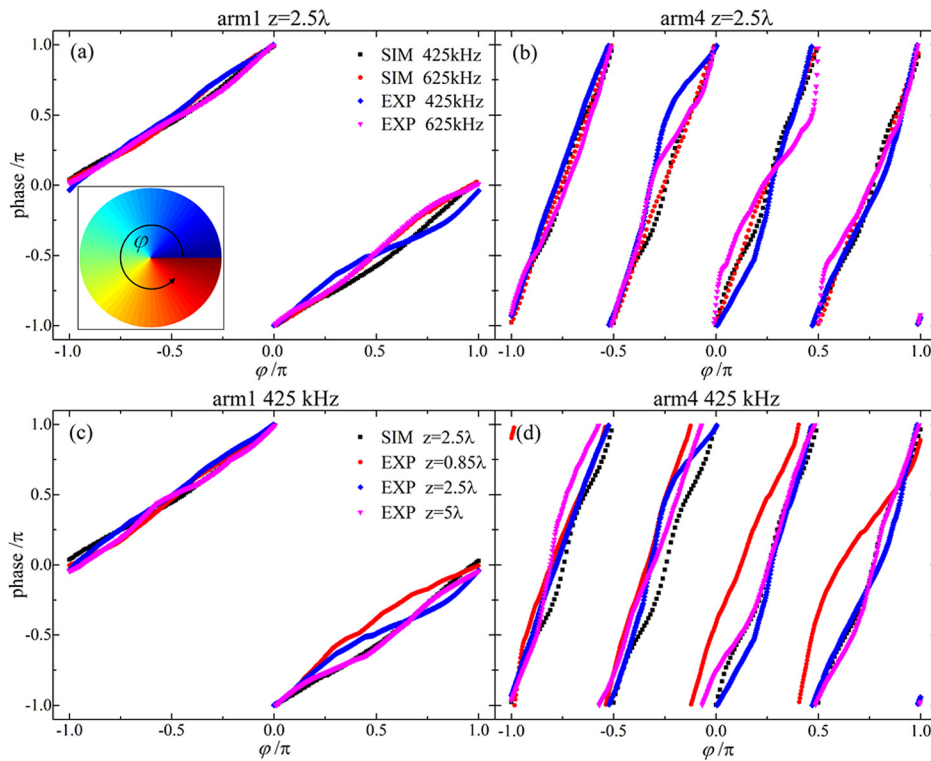


FIG. 4. (a) and (b) Relationships between the azimuthal angle ϕ and the phase variation in an annular loop around the singularity for the one-armed and four-armed coiling slits in 425 kHz and 625 kHz. (c) and (d) Simulated and measured relationships between ϕ and the phase in an annular loop around the singularity for the one-armed and four-armed coiling slits in 425 kHz at different propagation distances. Inset: schematic of the measurements.

example, the largest and smallest widths of the one-armed coiling split are 2.47 mm and 1 mm, which determine that the corresponding low and high critical frequencies of the structure are 305 kHz and 750 kHz, covering about 1.3 octaves. For the better demonstration of the stability and broadband functionality of the proposed MACS, we plot the relationships between the azimuthal angle ϕ and the phase variation in an annular loop around the singularity in different operating frequencies and propagation distances, and the measurements are schematically shown in the inset of Fig. 4(a). The comparisons between the simulations and the experimental results in different operating frequencies for the one-armed and four-armed structures are illustrated in Figs. 4(a) and 4(b). It can be clearly observed that both the simulated and the measured phases in 425 kHz and 625 kHz have shifted 2π (8π) for the one-armed (four-armed) structure, which demonstrate that the generation of acoustic vortices by the MACS is independent of the operating frequency. In addition, stability and sustenance of the topological charge is verified by comparing the numerical simulations and experimental results in different propagation distances for the one-armed and four-armed structures as shown in Figs. 4(c) and 4(d). The results distinctly display the phase variations as expected, which prove that the proposed MACS possess the unique characteristic of stable topological charge in a considerably long distance in the propagation direction.

We have proposed a broadband stable acoustic vortices generator based on the MACS in combination with the theoretical calculations, numerical simulations, and experimental verifications. The MACS-based generator is capable of spiraling the acoustic wave spatially and producing the twisted stable acoustic vortices by modulating the amplitude and phase of the wave in the diffraction field. The stability and sustenance of the topological charge is verified through both simulations and experiments, which can be

extended to a relatively long distance in the propagation direction for all the cases from one-armed to four-armed coiling slits. Moreover, the intrinsic broadband functionality is confirmed at different operating frequencies. With the controllable stable topological charge, broadband functionality, and exemption of the limitation of discretization precision, the MACS-based scheme is an effective alternate to generate the acoustic vortices, which may have potential applications, such as transportation and manipulation of small particles in acoustic tweezer, ultrasound therapy, imaging, and so on.

This work was supported by the National Basic Research Program of China (973 Program) (Grant Nos. 2011CB707900 and 2012CB921504), National Natural Science Foundation of China (Grant Nos. 11174138, 11174139, 11222442, 81127901, and 11274168), NCET-12-0254, and a project funded by the Priority Academic Program Development of Jiangsu Higher Education Institutions.

¹J. F. Nye and M. V. Berry, *Proc. R. Soc. London, Ser. A* **336**, 165 (1974).

²J. L. Thomas and R. Marchiano, *Phys. Rev. Lett.* **91**, 244302 (2003).

³P. L. Marston, *J. Acoust. Soc. Am.* **124**, 2905 (2008).

⁴P. L. Marston, *J. Acoust. Soc. Am.* **126**, 3539 (2009).

⁵L. K. Zhang and P. L. Marston, *Phys. Rev. E* **84**, 065601 (2011).

⁶C. R. P. Courtney, B. W. Drinkwater, C. E. M. Demore, S. Cochran, A. Grinenko, and P. D. Wilcox, *Appl. Phys. Lett.* **102**, 123508 (2013).

⁷C. R. P. Courtney, C. E. M. Demore, H. X. Wu, A. Grinenko, P. D. Wilcox, S. Cochran, and B. W. Drinkwater, *Appl. Phys. Lett.* **104**, 154103 (2014).

⁸A. L. Bernassau, C. R. P. Courtney, J. Beeley, B. W. Drinkwater, and D. R. S. Cumming, *Appl. Phys. Lett.* **102**, 164101 (2013).

⁹L. K. Zhang and P. L. Marston, *J. Acoust. Soc. Am.* **136**, 2917 (2014).

¹⁰G. T. Silva, *J. Acoust. Soc. Am.* **136**, 2405 (2014).

¹¹B. T. Hefner and P. L. Marston, *J. Acoust. Soc. Am.* **103**, 2971 (1998).

¹²B. T. Hefner and P. L. Marston, *J. Acoust. Soc. Am.* **106**, 3313 (1999).

- ¹³K. Volke-Sepulveda, A. O. Santillan, and R. R. Boullosa, [Phys. Rev. Lett.](#) **100**, 024302 (2008).
- ¹⁴K. D. Skeldon, C. Wilson, M. Edgar, and M. J. Padgett, [New J. Phys.](#) **10**, 013018 (2008).
- ¹⁵C. E. M. Demore, Z. Y. Yang, A. Volovick, S. Cochran, M. P. MacDonald, and G. C. Spalding, [Phys. Rev. Lett.](#) **108**, 194301 (2012).
- ¹⁶A. Anhauser, R. Wunenburger, and E. Brasselet, [Phys. Rev. Lett.](#) **109**, 034301 (2012).
- ¹⁷Z. Y. Hong, J. Zhang, and B. W. Drinkwater, [Phys. Rev. Lett.](#) **114**, 214301 (2015).
- ¹⁸D. Baresch, J.-L. Thomas, and R. Marchiano, [Phys. Rev. Lett.](#) **116**, 024301 (2016).